

## SEARCH FOR CO OUTFLOWS TOWARD A SAMPLE OF 69 HIGH-MASS PROTOSTELLAR CANDIDATES: FREQUENCY OF OCCURRENCE

QIZHOU ZHANG,<sup>1</sup> T. R. HUNTER,<sup>1</sup> J. BRAND,<sup>2</sup> T. K. SRIDHARAN,<sup>1</sup> S. MOLINARI,<sup>3</sup> M. A. KRAMER,<sup>4</sup> AND R. CESARONI<sup>5</sup>

*Received 2001 February 27; accepted 2001 April 10; published 2001 May 2*

### ABSTRACT

A survey for molecular outflows was carried out by mapping the CO  $J = 2-1$  line toward a sample of 69 luminous *IRAS* point sources. Sixty objects have *IRAS* luminosities from  $10^3$  to  $10^5 L_\odot$  and are associated with dense gas traced by  $\text{NH}_3$ , identifying them as high-mass star-forming regions. Among 69 sources, 65 sources have data that are suitable for outflow identification. Thirty-nine regions show spatially confined high-velocity wing emission in CO, indicative of molecular outflows. Most objects without identifiable outflows lie within  $0^\circ < l < 50^\circ$  where outflow signatures are confused by multiple cloud components along the line of sight. Excluding 26 sources with  $0^\circ < l < 50^\circ$ , we found 35 outflows out of 39 sources, which yields an outflow detection rate of 90%. Many of the outflows contain masses of more than  $10 M_\odot$  and have momenta of a few hundred  $M_\odot \text{ km s}^{-1}$ , at least 2 orders of magnitude larger than those in typical low-mass outflows. This class of massive and energetic outflows is most likely driven by high-mass young stellar objects. The high detection rate indicates that molecular outflows are common toward high-mass young stars. Given the connection between outflows and accretion disks in low-mass stars, we suggest that high-mass stars may form via an accretion-outflow process, similar to their low-mass counterparts.

*Subject headings:* accretion, accretion disks — H II regions — ISM: clouds — ISM: jets and outflows — stars: formation

### 1. INTRODUCTION

Molecular outflows mark an important phase in the early evolution of low-mass star formation (see Bachiller 1996 for a review). Observations accumulated over the past 20 years have shown that outflows are ubiquitous toward low-mass young stellar objects (YSOs). It is now believed that outflows are intimately related to the accretion process, play an important role in dissipating excess angular momentum in the infalling material, and allow the star to build up its mass through accretion. Molecular outflow is one of the essential building blocks in the understanding of low-mass star formation (e.g., Shu, Adams, & Lizano 1987).

Although it is generally agreed that high-mass stars ( $M > 8 M_\odot$ ) are often (and perhaps always) found in dense clusters (Stahler, Palla, & Ho 2000), there are opposing views regarding their formation. It has been shown that a protostellar core, once it reaches about  $10 M_\odot$ , can exert enough radiation pressure to halt spherical infall and inhibit further growth of the core mass (Wolfire & Cassinelli 1987). This led to one view that high-mass stars form by the coalescence of low- to intermediate-mass stars (Bonnell, Bate, & Zinnecker 1998). The other view is that since the dynamical processes near the (proto)star are not isotropic, high-mass stars could still form via infall and accretion. Currently, few observational constraints exist to discriminate between the two. Because of the connection between outflow and accretion seen in low-mass stars, surveys of molecular outflows in high-mass YSOs can shed light on this debate.

Outflows have been found toward regions where high-mass stars are formed (Kwan & Scoville 1976; Rodríguez, Ho, &

Moran 1980). However, the effort of searching for outflows has been hindered greatly by the large distances to these objects, the presence of multiple YSOs in the region, and the confusion due to clouds along the line of sight. There have been several surveys of molecular outflows toward luminous *IRAS* sources or ultra-compact H II regions. Broad wings of CO emission are found in a large fraction (between 40% and 90%) of the objects in the samples (Snell et al. 1988; Snell, Dickman, & Huang 1990; Wilking et al. 1989; McCutcheon et al. 1991; Shepherd & Churchwell 1996; Osterloh, Henning, & Launhardt 1997; T. K. Sridharan et al. 2001, in preparation). However, in most of the previous surveys, the objects were not mapped to the full spatial extent of the wing emission. Because of the complexity of these objects, it is conceivable that two cloud components can produce non-Gaussian line profiles that mimic wing emission. In addition, outflows can be offset from the *IRAS* position and, hence, would not be detected with a single spectrum toward the *IRAS* source. Thus, the rate of occurrence of molecular outflows in high-mass star-forming regions is not known.

In this Letter, we present a survey of a flux-limited sample of 69 *IRAS* point sources with infrared colors similar to compact molecular clouds (Richards et al. 1987). A significant improvement over the previous surveys is that we *mapped* the objects in the higher CO transition of  $J = 2-1$ . The statistics of the survey is presented in this Letter, while a detailed analysis of outflow properties will be presented in a future paper.

### 2. SAMPLE

We adopted the entire sample of high-mass young stars in Molinari et al. (1998a). This sample of 69 objects is selected from a complete flux-limited sample of the 260 *IRAS* point sources that satisfy flux, color, and practical requirements (Palla et al. 1991):  $F_{60 \mu\text{m}} \geq 100 \text{ Jy}$ ,  $0.61 \leq \log(F_{60 \mu\text{m}}/F_{25 \mu\text{m}}) \leq 1.74$ , and  $0.087 \leq \log(F_{100 \mu\text{m}}/F_{60 \mu\text{m}}) \leq 0.52$ ; Galactic latitude  $|b| \leq 10^\circ$ ; they should not have upper limits at 25, 60, and  $100 \mu\text{m}$ ; they should have no positional coincidence with known H II regions; and  $\delta \geq -30^\circ$ . The far-IR color criteria were chosen so

<sup>1</sup> Harvard-Smithsonian Center for Astrophysics, 60 Garden Street, Cambridge, MA 02138.

<sup>2</sup> Istituto di Radioastronomia, CNR, via Gobetti 101, Bologna, I-40129, Italy.

<sup>3</sup> Istituto di Fisica dello Spazio Interplanetario, CNR, 100 via del Fosso del Cavaliere, Roma, I-00133, Italy.

<sup>4</sup> Oberlin College, Mailroom Box 1634, Oberlin, OH 44074.

<sup>5</sup> Osservatorio Astronomico di Arcetri, Largo Enrico Fermi 5, Firenze, I-50125, Italy.

that the sample has colors similar to compact molecular clouds (Richards et al. 1987). Among the 260 sources in the original sample, 125 have colors similar to the ultracompact H II regions (Wood & Churchwell 1989) and were termed the “*high*” group. The remaining 135 objects in the sample were termed the “*low*” group (Palla et al. 1991). The original sample has been studied in H<sub>2</sub>O masers (Palla et al. 1991) with the Medicina 32 m telescope and in NH<sub>3</sub> with the Effelsberg 100 m telescope (Molinari et al. 1996). The candidate high-mass (proto)stars, a subset of the original sample, were mapped in 2 and 6 cm with the VLA (Molinari et al. 1998a) and with millimeter and submillimeter wavelengths (Molinari et al. 2000). Various indicators, such as gas temperatures and NH<sub>3</sub> line widths, the detection rate of H<sub>2</sub>O masers, and radio continuum, suggest that objects in the *low* group are at an earlier evolutionary stage than those in the *high* group (Palla et al. 1991; Molinari et al. 1996, 1998a, 2000).

### 3. OBSERVATIONS AND DATA REDUCTION

#### 3.1. NRAO 12 m Telescope

During the winter of 1998 and 1999, observations of the CO  $J = 2-1$  transition were made using the 12 m telescope of the National Radio Astronomy Observatory<sup>6</sup> at Kitt Peak. In the winter of 1998, we used the 1 mm SIS array receiver (Payne & Jewell 1995) that consists of  $2 \times 4$  independent beams. The hybrid-correlator spectrometer was set at a bandwidth of 150 MHz, yielding a frequency resolution of 781.2 kHz or a velocity resolution of  $1.02 \text{ km s}^{-1}$  for the CO  $J = 2-1$  transition frequency. The typical integration time on each position was about 4 minutes, giving an rms of about  $T_A^* = 0.08 \text{ K}$  with a system temperature of  $\approx 700 \text{ K}$ .

In 1999, we used the 1 mm dual-channel SIS receiver and the newly commissioned Millimeter Autocorrelator spectrometer with a 75 MHz/150 MHz bandwidth split into 16,384 channels. We smoothed the data during data reduction to a resolution of  $0.5 \text{ km s}^{-1}$  per channel. Data of both polarizations were taken and averaged to increase the signal-to-noise ratio. The typical integration time on each position is about 1 minute. With lower receiver temperatures than the 8 beam receiver and the dual polarizations, the rms in the averaged spectra is comparable to those in the 1998 data. All the 12 m maps were acquired at a  $29''$  spatial sampling, approximately the resolution of the telescope at the CO  $J = 2-1$  frequency. The main-beam efficiency is about 30%.

To ensure flat baselines in the spectra, all the data were taken in position-switching mode. Because of the large spatial coverage and sensitivity of the array receiver, most reference positions suggested in the literature have detectable CO emission and were not suitable as references here. We therefore sought for “clean” reference positions (i.e., no detectable signal at the LSR velocity of the object at the designated rms level) in nearby regions with the same Galactic longitude as the target source and a few degrees off the Galactic plane. The clean off-positions are normally  $2^\circ-4^\circ$  from the source. Typically, the baselines were flat and suitable for discerning outflow signatures. Data reduction was performed using the CLASS package.

<sup>6</sup> The National Radio Astronomy Observatory is operated by Associated Universities, Inc., under cooperative agreement with the National Science Foundation.

#### 3.2. Caltech Submillimeter Observatory Telescope

A subset of the sample was observed at the Caltech Submillimeter Observatory in July and October of 1997 as backup projects when the weather was not suitable for observations at higher frequencies. Eight sources were observed in the CO  $J = 2-1$  line. The maps of the CO  $J = 2-1$  line were obtained with a  $30''$  grid spacing, approximately the angular resolution of the telescope at that frequency. The typical system temperature at the CO  $J = 2-1$  line was about 400 K. The rms in the spectra is about 0.05 K in  $T_A^*$  per  $0.3 \text{ km s}^{-1}$  channel. The main-beam efficiency is about 75%.

## 4. RESULTS AND DISCUSSION

### 4.1. Identification of Outflows

A typical outflow appears as spatially confined wings beyond the emission from the cloud core. This signature is sought for in the grid map of CO spectra and the position-velocity diagram. The position-velocity diagram can be particularly revealing when there are multiple velocity components blended closely together in velocity. The position-velocity plots were also used to determine the velocity range of outflowing gas. We then make maps of integrated CO emission to confirm that the wing emission is spatially confined. Figure 1 shows the integrated emission (Fig. 1a) and the position-velocity plot (Fig. 1b) for IRAS 05137+3917 as an example.

### 4.2. Outflow Detection Rate

Using the procedure outlined above, we identified 39 molecular outflows in the sample of 65 sources that have data suitable for outflow identification. This gives an outflow detection rate of 60%. Table 1 summarizes the results for objects in different categories. Figure 2a presents the distribution of the objects in Galactic coordinates. It is apparent that the outflow objects are located predominantly in the region with  $50^\circ < l < 240^\circ$ . Within this region, there are 35 outflow sources out of 39 objects. This gives an outflow detection rate of 90%. Toward the region with  $0^\circ < l < 50^\circ$ , there are four detected outflow sources out of 26 objects, which represents a detection rate of 15%.

The kinematic distance and luminosity of the objects in the sample are shown in Figures 2b and 2c, respectively. The lu-

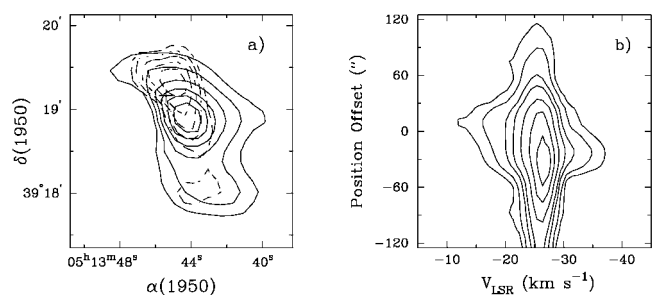


FIG. 1.—(a) Integrated emission map and (b) position-velocity plot of the CO  $J = 2-1$  line for IRAS 05137+3919. The range of integration is from  $-28$  to  $-40 \text{ km s}^{-1}$  for the blue lobe (solid contours) and from  $10$  to  $-23 \text{ km s}^{-1}$  for the red lobe (dashed contours), respectively. The contour levels in (a) are at every  $8 \text{ K (km s}^{-1})$  starting from  $24 \text{ K (km s}^{-1})$ . The cross denotes the position of the IRAS source. The contour levels in (b) are at 1, 2, 4, 6, 10, and  $15 \text{ K}$ . The cut for the position-velocity plot is along the peaks of the blue and red lobes.

minosity is computed from the *IRAS* fluxes and the kinematic distance. As seen in Figure 2*b*, the average distance for sources with  $0^\circ < l < 50^\circ$  is similar to that with  $l > 50^\circ$ . In addition, the luminosities for the two groups are similar. Therefore, the lack of molecular outflow detections toward the objects with  $0^\circ < l < 50^\circ$  is probably not due to the large distances to the sources, or to the effect of luminosity, but to the presence of multiple velocity components along the line of sight toward the Galactic molecular ring. Nearly all sources without outflow identification have multiple cloud components that are blended together. Under such circumstances, the outflow signatures are obscured by emission from clouds at slightly different velocities. Thus, the detection rate of 90% derived for objects with  $l > 50^\circ$  is representative of the whole sample.

In the sample, there are nine sources with luminosities less than  $10^3 L_\odot$ , a conventional criterion to separate high-mass stars from the low- to intermediate-mass stars. We did not exclude them when computing the detection statistics because many sources with low luminosities have large uncertainties in distance and thus in luminosity. The outflow detection rate remains the same if these sources are excluded from the statistics.

Outflow detections for subsamples according to the *low* and *high* classification and the occurrence of  $\text{H}_2\text{O}$  masers are given in Table 1. The number of objects in some subgroups is small, and the statistics may not be significant. In addition, samples with  $0^\circ < l < 50^\circ$  are contaminated by complex CO spectra. Overall, outflows are detected in both the *low* and *high* groups. Furthermore, outflow detection rates are higher (see Table 1) in objects with  $\text{H}_2\text{O}$  masers. This result is consistent with the notion

that molecular outflows and  $\text{H}_2\text{O}$  masers are connected. However, it is interesting to point out that 16 CO outflows are found in 36 objects with no detectable  $\text{H}_2\text{O}$  masers. This result suggests that outflows may develop before the appearance of  $\text{H}_2\text{O}$  masers.

### 4.3. Masses and Momenta in Outflows

In computing the outflow mass, we adopt a CO abundance  $[\text{CO}/\text{H}_2] = 10^{-4}$  (Frerking, Langer, & Wilson 1982). We also assume that the CO line wings are optically thin. We use the line-of-sight velocity when calculating the momentum. Because the wing emission can be partially optically thick and the outflow axis is not necessarily along the line of sight, both quantities are lower limits.

Figure 3 presents the distribution of outflow masses and momenta for the 30 high-mass YSOs ( $L > 10^3 L_\odot$ ) for which the outflow parameters can be determined. We excluded objects with  $L < 10^3 L_\odot$  because of the uncertainty in the kinematic distance and, hence, the outflow mass. Nineteen outflows have masses greater than  $10 M_\odot$ . The remaining 11 have masses from 1 to  $10 M_\odot$ . Nineteen of the flows have momenta greater than  $50 M_\odot (\text{km s}^{-1})$ . Thirteen of them have momenta greater than  $100 M_\odot (\text{km s}^{-1})$ . These results can be compared with a similar study conducted toward 45 low-mass YSOs with luminosities of  $0.4\text{--}26 L_\odot$  (Bontemps et al. 1996); without the correction for the optical depth effect and inclination angle of the outflow, the momenta are all less than  $1 M_\odot (\text{km s}^{-1})$ , with typical values of  $0.1 M_\odot (\text{km s}^{-1})$ .

The large masses and momenta in these outflows indicate that the outflows in high-mass star-forming regions may be different from those associated with low-mass stars. What is the engine driving those massive molecular outflows? For most of the outflows in our sample, we found that the *IRAS* source is located at/near the center of the flow. This indicates that the high-mass star is likely to be the driving source of the outflow. However, since high-mass stars typically form in a cluster with stars of lower masses, it remains possible that massive outflows are driven by low-mass YSOs in the cluster. A single low-mass star cannot power the massive outflow since a typical outflow associated with a low-mass star has a momentum at least 2 orders of magnitude lower than those observed here. Could high-mass outflows be powered by a *group* of low-mass stars? This scenario would require the alignment of the outflow axes and the polarity of a large number of low-mass YSOs. Such an alignment has not been observed even in binary systems such as L1551 IRS 5 in which the two jets are about  $30^\circ$  apart

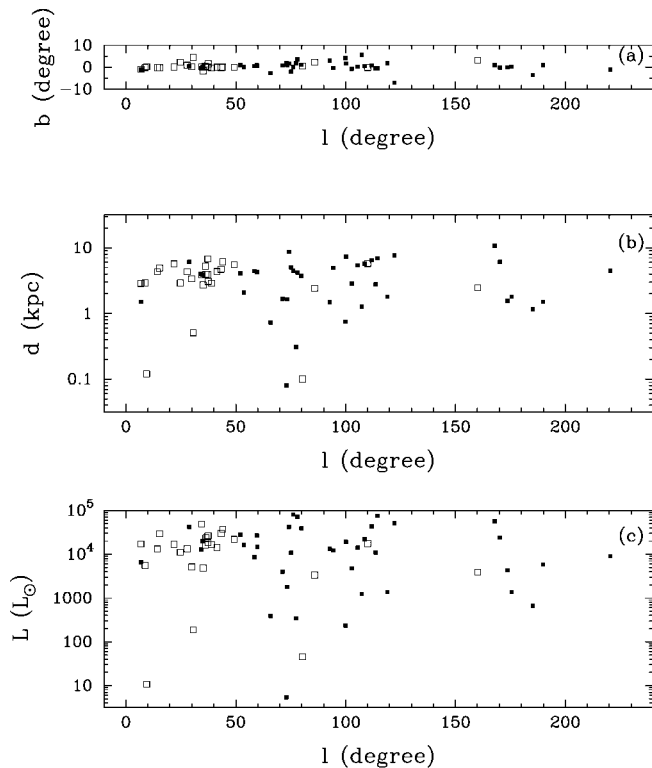


FIG. 2.—Distribution of the sample in (a) Galactic coordinates, (b) kinematic distances, and (c) luminosity. The filled squares are the *IRAS* point sources with identifiable outflows. The open squares are the *IRAS* point sources without identifiable outflows.

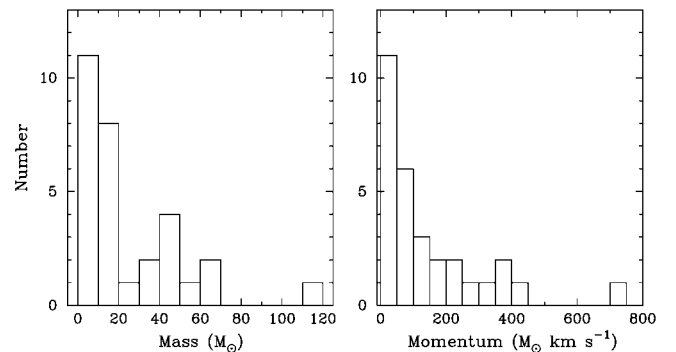


FIG. 3.—Distribution of outflow mass and momentum for 30 objects with luminosities greater than  $10^3 L_\odot$  and for which reliable mass estimates are determined.

TABLE 1  
CO OUTFLOW DETECTION RATE

CATEGORY	NUMBER OF OUTFLOWS AND DETECTION RATE <sup>a</sup>		
	$l < 50^\circ$	$l > 50^\circ$	Total
Total .....	4/26	35/39 (90%)	39/65
High .....	1/7	22/24 (92%)	23/31
Low .....	3/19	13/15 (87%)	16/34
With H <sub>2</sub> O:			
High .....	0/2	16/17 (94%)	16/19
Low .....	0/3	7/7 (100%)	7/10
Without H <sub>2</sub> O:			
High .....	1/5	6/7 (86%)	7/12
Low .....	3/16	6/8 (75%)	9/24

<sup>a</sup> The outflow detection rate toward  $0^\circ < l < 50^\circ$  may not be representative because of the confusion in CO spectra by multiple cloud components along the line of sight.

in projection (Itoh et al. 2000). Thus, it is most likely that the high-mass YSOs are responsible for the massive outflows.

The direct association of molecular outflows with their driving sources requires high angular resolution mapping. In five sources of the sample observed with interferometers (Molinari et al. 1998b; Hunter et al. 1999; Cesaroni et al. 1999; Shepherd et al. 2000), the core in which the high-mass (proto)star is embedded is located at the center of the outflow. Observations of outflows toward other high-mass young stars also confirm such an association (Shepherd et al. 1998; Gómez et al. 1999).

#### 4.4. Implications for High-Mass Star Formation

The high detection rate of molecular outflows in high-mass young stars implies that molecular outflows are common to-

ward high-mass YSOs. This has interesting implications for how high-mass stars are formed. Studies of low-mass YSOs have suggested that infall and accretion processes drive the outflow. The infalling/accreting material with excess angular momentum escapes the gravitational potential of the star and is directed to the polar axis of the accretion disk (e.g., Shu et al. 2000). The widespread existence of molecular outflows in high-mass YSOs suggests that high-mass stars may also form through infall and accretion. Similar to low-mass stars, disks and jetlike outflows have been detected toward high-mass stars (Cesaroni et al. 1997, 1999; Zhang, Hunter, & Sridharan 1998; Zhang et al. 1999; Hunter et al. 1999). Detailed models are required to understand the driving mechanism of molecular outflows in high-mass stars (Churchwell 1997; Königl 1999).

#### 5. CONCLUSIONS

We present a survey of CO outflows toward a sample of the flux-limited *IRAS* point sources. Most objects in the sample are luminous ( $10^3$ – $10^5 L_\odot$ ), high-mass young stars. Excluding the objects with  $0^\circ < l < 50^\circ$  where confusion by clouds along the line of sight dominates the CO spectra, we found 90% of the sample to possess molecular outflows. The outflows are massive, typically having masses of more than  $10 M_\odot$ . This unbiased survey suggests that outflows are common in high-mass stars and can appear even before the H<sub>2</sub>O maser phase. Drawing analogies to the low-mass counterparts, we suggest that high-mass stars may form via an accretion-outflow process, similar to the low-mass stars.

We are grateful to the NRAO 12 m telescope operators who helped us during many long sessions of observations.

#### REFERENCES

- Bachiller, R. 1996, *ARA&A*, 34, 111  
 Bonnell, I., Bate, M. R., & Zinnecker, H. 1998, *MNRAS*, 298, 93  
 Bontemps, S., André, P., Terebey, S., & Cabrit, S. 1996, *A&A*, 311, 858  
 Cesaroni, R., Felli, M., Jenness, T., Neri, R., Robberto, M., Testi, L., & Walmsley, C. M. 1999, *A&A*, 345, 949  
 Cesaroni, R., Felli, M., Testi, L., Walmsley, C. M., & Olmi, L. 1997, *A&A*, 325, 725  
 Churchwell, E. 1997, *ApJ*, 479, L59  
 Frerking, M. A., Langer, W. D., & Wilson, R. W. 1982, *ApJ*, 262, 590  
 Gómez, J. F., Sargent, A. I., Torrelles, J. M., Ho, P. T. P., Rodríguez, L. F., Cantó, J., & Garay, G. 1999, *ApJ*, 514, 287  
 Hunter, T. R., Testi, L., Zhang, Q., & Sridharan, T. K. 1999, *AJ*, 118, 477  
 Itoh, Y., et al. 2000, *PASJ*, 52, 81  
 Königl, A. 1999, *NewA Rev.*, 43, 67  
 Kwan, J., & Scoville, N. 1976, *ApJ*, 210, L39  
 McCutcheon, W. H., Dewdney, P. E., Purton, R., & Sato, T. 1991, *AJ*, 101, 1435  
 Molinari, S., Brand, J., Cesaroni, R., & Palla, F. 1996, *A&A*, 308, 573  
 ———. 2000, *A&A*, 355, 617  
 Molinari, S., Brand, J., Cesaroni, R., Palla, F., & Palumbo, G. G. C. 1998a, *A&A*, 336, 339  
 Molinari, S., Testi, L., Brand, J., Cesaroni, R., & Palla, F. 1998b, *ApJ*, 505, L39  
 Osterloh, M., Henning, Th., & Launhardt, R. 1997, *ApJS*, 110, 71  
 Palla, F., Brand, J., Comoretto, G., Felli, M., & Cesaroni, R. 1991, *A&A*, 246, 249  
 Payne, J. M., & Jewell, P. R. 1995, in *ASP Conf. Ser. 75, Multi-Feed Systems for Radio Telescopes*, ed. D. T. Emerson & J. M. Payne (San Francisco: ASP), 144  
 Richards, P. J., Little, L. T., Toriseva, M., & Heaton, B. D. 1987, *MNRAS*, 228, 43  
 Rodríguez, L. F., Ho, P. T. P., & Moran, J. M. 1980, *ApJ*, 240, L149  
 Shepherd, D. S., & Churchwell, E. 1996, *ApJ*, 472, 225  
 Shepherd, D. S., Watson, A. M., Sargent, A. I., & Churchwell, E. 1998, *ApJ*, 507, 861  
 Shepherd, D. S., Yu, K. C., Bally, J., & Testi, L. 2000, *ApJ*, 535, 833  
 Shu, F. H., Adams, F. C., & Lizano, S. 1987, *ARA&A*, 25, 23  
 Shu, F. H., Najita, J. R., Shang, H., & Li, Z.-Y. 2000, in *Protostars and Planets IV*, ed. V. Mannings, A. P. Boss, & S. S. Russell (Tucson: Univ. Arizona Press), 789  
 Snell, R. L., Dickman, R. L., & Huang, Y.-L. 1990, *ApJ*, 352, 139  
 Snell, R. L., Huang, Y.-L., Dickman, R. L., & Claussen, M. J. 1988, *ApJ*, 325, 853  
 Stahler, S. W., Palla, F., & Ho, P. T. P. 2000, in *Protostars and Planets IV*, ed. V. Mannings, A. P. Boss, & S. S. Russell (Tucson: Univ. Arizona Press), 327  
 Wilking, B. A., Mundy, L. G., Blackwell, J. H., & Howe, J. E. 1989, *ApJ*, 345, 257  
 Wolfire, M. G., & Cassinelli, J. P. 1987, *ApJ*, 319, 850  
 Wood, D. O. S., & Churchwell, E. 1989, *ApJS*, 69, 831  
 Zhang, Q., Hunter, T. R., & Sridharan, T. K. 1998, *ApJ*, 505, L151  
 Zhang, Q., Hunter, T. R., Sridharan, T. K., & Cesaroni, R. 1999, *ApJ*, 527, L117